Contribution of Wolf-Rayet stars to the synthesis of ^{26}Al

I. The γ-ray connection

G. Meynet[1], **M. Arnould**[2], **N. Prantzos**[3,4], **and G. Paulus**[2]

[1] Observatoire de Genève, CH-1290 Sauverny, Switzerland
[2] Institut d'Astronomie et d'Astrophysique, Université Libre de Bruxelles, CP 226, Campus Plaine, Bd. du Triomphe,
    B-1050 Bruxelles, Belgium
[3] Institut d'Astrophysique de Paris, 98bis Bd. Arago, F-75014 Paris, France
[4] Service d'Astrophysique, DAPNIA, CE Saclay, F-91191 Gif-sur-Yvette, France

Abstract. New ^{26}Al yield predictions are derived from Wolf-Rayet (WR) model stars that are able to account better than previous ones for many important observed characteristics (like luminosities, surface chemical compositions, or number statistics) as a result of the adoption of new physical ingredients, and in particular of higher mass loss rates. The updated yields computed for WR stars with initial masses between 25 and 120 $M_\odot$ and metallicities $Z = 0.008$, 0.020, and 0.040, turn out to be about twice larger than previously reported ones.

These WR yields lead to a galactic steady state ^{26}Al production rate of $0.9 \pm 0.5\, M_\odot\, \text{My}^{-1}$. The quoted error bar just takes into account the uncertainties in the IMF slope, the galactic metallicity gradient and the core collapse supernova rate. Thus, WR stars might account for 20 to 70% of the approximate 2 $M_\odot$ of ^{26}Al that are believed to be present in our Galaxy.

An even larger ^{26}Al contamination of the Galaxy by WR stars cannot be ruled out, as it appears from an analysis of the impact on the ^{26}Al yields of other sources of uncertainty that affect individual model stars, like the mass loss rate, the mixing procedure, and some key nuclear reaction rates. Each effect considered separately may lead to an additional uncertainty in the WR yields that amounts to a factor of about 2 to 3.

Key words: stars: Wolf-Rayet – gamma-rays: theory – nucleosynthesis, abundances

1. Introduction

The many observations of the emission of a 1.809 MeV γ–ray line from the galactic disk (see Prantzos & Diehl 1996 for a recent review) provide ample evidence that it contains about

Send offprint requests to: G. Meynet

2 $M_\odot$ of recently synthesized ^{26}Al ($t_{1/2} = 7.3\,10^5$ y). In addition, a wealth of observations demonstrate that ^{26}Al has decayed in situ in some meteoritic inclusions of solar origin (as reviewed by MacPherson et al. 1995), or in various meteoritic grains of likely circumstellar origin (see Anders & Zinner 1993).

These astronomical and cosmochemical observations clearly raise, among many others, the question of the nucleosynthetic origin of ^{26}Al. As reviewed by Prantzos & Diehl (1996), asymptotic giant branch stars, Wolf-Rayet (WR) stars, novae, supernovae, and spallation reactions in interstellar clouds have been envisioned.

This paper aims at revisiting the ^{26}Al yields based on models for WR stars that account better than previous ones for many observable properties of this type of stars, like their luminosities, surface chemical compositions, or statistics in regions of constant star formation rate, as well as in starburst locations. This improved agreement is obtained through progress made recently in our knowledge of several key physical ingredients, like the opacities, mass loss rates, or nuclear reaction rates. These revised stellar models are described in Sect. 2. The resulting ^{26}Al yields from individual model stars are presented in Sects. 3, while the global contribution of the WR stars to the galactic ^{26}Al is estimated in Sect. 4. Conclusions are drawn in Sect. 5.

2. The WR model stars

Stars with initial masses M_i in excess of some critical value (around 25 to 30 $M_\odot$ for a Pop I composition) are expected to go through the WR phase. Due to strong winds, the original stellar envelope may be removed, so that the H-burning (CNO processed) core may appear at the stellar surface, leading to the development of the WN phase (comprising the WNL and WNE sub-phases). This stage is considered to start when the surface hydrogen mass fraction decreases below 0.4 and the effective temperature $\log T_{eff}$ exceeds about 4 (cf. Schaller et al. 1992). In at least certain cases, the further peeling-off of the

star may transform the WN star into a WC-WO object. The WC phase starts when He-burning products appear at the surface. The star may then evolve into the WO phase when the ratio $(X_C + X_O)/X_{He}$ increases above unity (Smith & Maeder 1991), X_C, X_O and X_{He} being the carbon, oxygen and helium mass fractions. In the following, no distinction will be made between the WC and WO phases. The important WR enrichment of the interstellar medium with H-burning products (especially ^{26}Al), as well as with He-burning ashes, at least if the star can reach the WC-WO stage, may have important astrophysical consequences. This paper just deals with the possible contribution of WR stars to the galactic 1.8 MeV γ-ray luminosity from the ^{26}Al decay.

2.1. Improved physical ingredients

There are some good reasons to update previous ^{26}Al yield predictions based on a large grid of WR models (Walter & Maeder 1989, Prantzos 1991). This comes about because of some important improvements brought recently to many key physical ingredients of the models. These are taken into account in the computations reported in this paper and are briefly described below:

(1) use is made of the new radiative opacity estimates provided by Iglesias & Rogers (1993);

(2) for consistency, our solar metallicity ($Z = Z_\odot$) models are assumed to have the same initial mixture of C to Fe elements as the one adopted for the opacity calculations (see Table 3 of Iglesias & Rogers 1993), while the H and He mass fractions are assumed to be $X = 0.68$ and $Y = 0.30$. In addition, the isotopic composition is adopted from Anders & Grevesse (1989). For $Z \neq Z_\odot$, the metal abundances are just scaled by the factor $Z/Z_\odot$;

(3) within the framework of the Schwarzschild criterion for convection and of a moderate core overshooting[1] adopted in this and previous work (e.g. Schaller et al. 1992), the models cannot account for several observed features if use is made of the pre-WR and WNL mass loss rates of de Jager et al. (1988) and Abbott and Conti (1987), respectively. A much better agreement between theory and observation is achieved when mass loss rates that are twice the values given by these authors are adopted (Meynet et al. 1994; Maeder & Meynet 1994). These enhanced stellar winds are also adopted in this paper. For WNE and WC stars, we adopt the mass dependence of $\dot{M}$ proposed by Langer (1989), as in Schaller et al. (1992).

The assumed metallicity dependence of the stellar wind has been shown to impact strongly on the calculated ratios WR/O and WC/WN of stellar types in galaxies of the Local Group (Maeder 1991). Following stellar wind model predictions (e.g. Kudritzki et al. 1987, 1991), the pre-WR mass loss rates are assumed here, as well as in the models of Schaller et al. (1992), to scale with metallicity Z as $\dot{M}(Z)/\dot{M}(Z_\odot) = (Z/Z_\odot)^{0.5}$;

(4) The nuclear reaction network for hydrogen burning used by Meynet et al. (1994) has been extended to the NeNa and MgAl

chains. It includes in particular the reactions leading to the production and destruction of the ^{26}Al ground (^{26}Al^g) and isomeric (^{26}Al^m) states, considered as two separate species at the temperatures of relevance to the WR model stars (Ward & Fowler 1980). Most of the H-burning rates are taken from Caughlan & Fowler (1988). When it appears, their (0-1) uncertainty factor is adopted equal to 0.1. Updated rates have, however, been used in some cases. The standard set includes the following rates: Landré et al. (1990) for ^{17}O (p, α) ^{14}N and ^{17}O (p, γ) ^{18}F, Kious (1990) for ^{19}F (p, α) ^{16}O, Illiadis et al. (1990) for ^{25}Mg (p, γ) ^{26}Al and ^{26}Mg (p, γ) ^{27}Al, Champagne et al. (1993) for ^{26}Al^g (p, γ) ^{27}Si, Champagne et al. (1988) for ^{27}Al (p, α) ^{24}Mg. A limited analysis of the impact on the ^{26}Al yields of the remaining uncertainties in the rates of some of these reactions is presented in Sect. 4.3.

The rates of the He-burning reactions are those adopted by Meynet & Arnould (1993a,b), except that the rate proposed by Giesen et al. (1994) is adopted for ^{18}O (α, γ) ^{22}Ne. In order to model correctly the s-process that develops during the WR core He-burning (to be discussed elsewhere), all the neutron sources and sinks up to ^{27}Al have been included in the nuclear network. The neutron poisoning by the heavier nuclides is approximated by an effective neutron sink (see e. g. Jorissen & Arnould 1989).

All the other physical ingredients are the same as in Meynet et al. (1994).

2.2. General characteristics of the models

The general properties of the present models do not differ substantially from those of Meynet et al. (1994). In particular, as in this earlier study, the "enhanced" stellar wind prescription mentioned above, leads to an improved agreement between predictions and several observed WR properties, as for instance their luminosities, their surface chemical composition, as well as the number ratio of WR to O type stars in zones of constant star formation rate and in starburst regions (Maeder & Meynet 1994; Meynet 1995).

Figs. 1 and 2 display the evolution of the total and convective core masses of various of the computed model stars. While Fig. 1 emphasizes the impact of a metallicity variation for $M_i = 60 \, M_\odot$, Fig. 2 describes the changes in the structural evolution when M_i varies at constant ($Z = Z_\odot$) metallicity. The different spectroscopic classes through which the displayed model stars evolve are also indicated.

For each of the computed model stars, Table 1 provides the lifetimes of the H- and He-burning phases, as well as of the WR stage and of the associated spectroscopic classes. The replacement of the opacities of Iglesias et al. (1992) used by Meynet et al. (1994) by those of Iglesias & Rogers (1993) used in the present models leads to somewhat shorter H-burning lifetimes due to slightly increased luminosities predicted during this burning phase. This reduction amounts to 20% and 10% for the 120 and 85 $M_\odot$ models with $Z = 0.04$, but is limited to less than 4% for the other models. In contrast, the He-burning lifetimes found here are about 10 to 30 % longer than those found by Meynet et al. (1994). This is a direct consequence of the smaller total masses of the stars when they enter the He-burning phase, this

---

[1] $d/H_p = 0.2$, where d is the overshooting distance and H_p the pressure scale height at the boundary of the classical core.

Table 1. Duration (in 10^6 y) of the various evolutionary phases of stars with metallicity Z and initial mass M_i.

$M_i(M_\odot)$	H-burning phase	He-burning phase	t(WR)	t(WNL)	t(WNE)	t(WC)
			$Z=0.008$			
120	2.8622	0.6979	1.1223	0.4381	0.0040	0.6802
85	3.1189	0.5525	0.6065	0.1685	0.0027	0.4353
60	3.6713	0.5884	0.5722	0.0905	0.0142	0.4675
40	4.6779	0.5632	0.1842	0.0369	0.0335	0.1138
			$Z=0.020$			
120	2.9695	0.9569	1.9642	1.0213	0.3078	0.6351
85	3.0315	0.8918	1.4118	0.5115	0.0857	0.8146
60	3.3495	0.6808	0.6758	0.0417	0.0172	0.6170
40	4.3314	0.6040[*1]	0.5582[*1]	0.0341	0.0660	0.4580[*1]
25	6.3848	0.7904[*2]	0.0000	0.0000	0.0000	0.0000
			$Z=0.040$			
120	3.9704	2.2903	4.8229	2.7953	2.0275	0.0000
85	3.1844	1.1160	2.3073	1.2564	1.0509	0.0000
60	3.1111	0.6871	1.0066	0.3086	0.1334	0.5646
25[*3]	5.5234	0.8364	0.5815	0.0523	0.1858	0.3434

Notes:
(1) The computations are stopped when the central helium mass fraction $Y = 0.0774$.
(2) The computations are stopped when $Y = 0.0025$.
(3) This model is computed with a slightly different initial composition and with the rate of Vogelaar (1989) for the reaction ^{26}Al^g(p,γ)^{27}Si. These changes have negligible effects on the values listed in this table (see text).

mass reduction being implied by the larger prior mass losses associated with the previously mentioned higher luminosities experienced during the H-burning stage.

The fate of the 120 and 85 $M_\odot$ with $Z = 0.040$ deserves some further comments. In these high metallicity cases, the peeling-off of the star by stellar winds is predicted to be so strong that these stars might end their lives as white dwarfs (Meynet et al. 1994). In addition, they spend their whole WR phase as WNL stars. This is also a consequence of the strong stellar winds. These indeed force such a drastic reduction of the main sequence convective core that the He-burning core becomes so small that it is never uncovered by the stellar winds.

3. Yields of ^{26}Al from WR stars

The production of ^{26}Al takes place during the core H-burning phase of the WR stars. It results from the MgAl chain operating at central temperatures between 35 and 45 10^6 K, while the central densities are of the order of a few g cm^{-3}. In such conditions, ^{26}Al is synthesized by proton captures on ^{25}Mg, and mainly destroyed by β^+-decay, the ^{26}Al^g (p , γ) ^{27}Si channel being much less probable. As a result, and as made clear in Figs. 1 and 2, the core ^{26}Al mass fraction X_{26}^c goes through a maximum $X_{26,\text{max}}^c$ at $t_M \approx \tau_{26}$, where τ_{26} is the ^{26}Al β-decay lifetime. The destruction of ^{26}Al is accelerated at the beginning of the He-burning phase as a result of ^{26}Al^g (n , p) ^{26}Mg neutron captures in the convective He-burning core. As a consequence, the late

WC-WO evolutionary phases cannot contribute to the ^{26}Al production (Prantzos & Cassé 1986).

3.1. Dependence of the yields on the initial mass and metallicity

In the nucleosynthesis pattern sketched above, a first Z-dependent effect concerns the importance of the ^{26}Al production channel, which increases with the initial amount of ^{25}Mg, and thus with metallicity. In contrast, its β-decay destruction is Z-independent. The net increase of the core ^{26}Al content with Z is illustrated in Fig. 1, where it is seen that $X_{26,\text{max}}^c$ increases by a factor of about 1.5 when Z is doubled.

A second consequence of a metallicity variation concerns the instant t_M at which $X_{26,\text{max}}^c$ is reached. Fig. 1 shows that this time increases with Z. For example, it goes from about $0.7 \, 10^6$ y to approximately $1.4 \, 10^6$ y when Z increases from 0.008 to 0.04. This effect relates directly to the fact that, for a given initial mass, a Z increase imposes a lower central temperature (due to greater CNO content), and consequently a slower building up of ^{26}Al at the beginning of the H-burning phase.

Finally, a Z variation has an impact on the evolution of the post-maximum X_{26}^c values. More specifically, Fig. 1 indicates that X_{26}^c decreases more slowly for higher metallicities. This effect relates to the smaller convective cores found at higher Z as a consequence of both lower central temperatures and stronger $\dot{M}$. The post-maximum X_{26}^c values are influenced by the extent of the convective core in the following way: convection mixes the innermost ^{26}Al-rich layers with zones that are
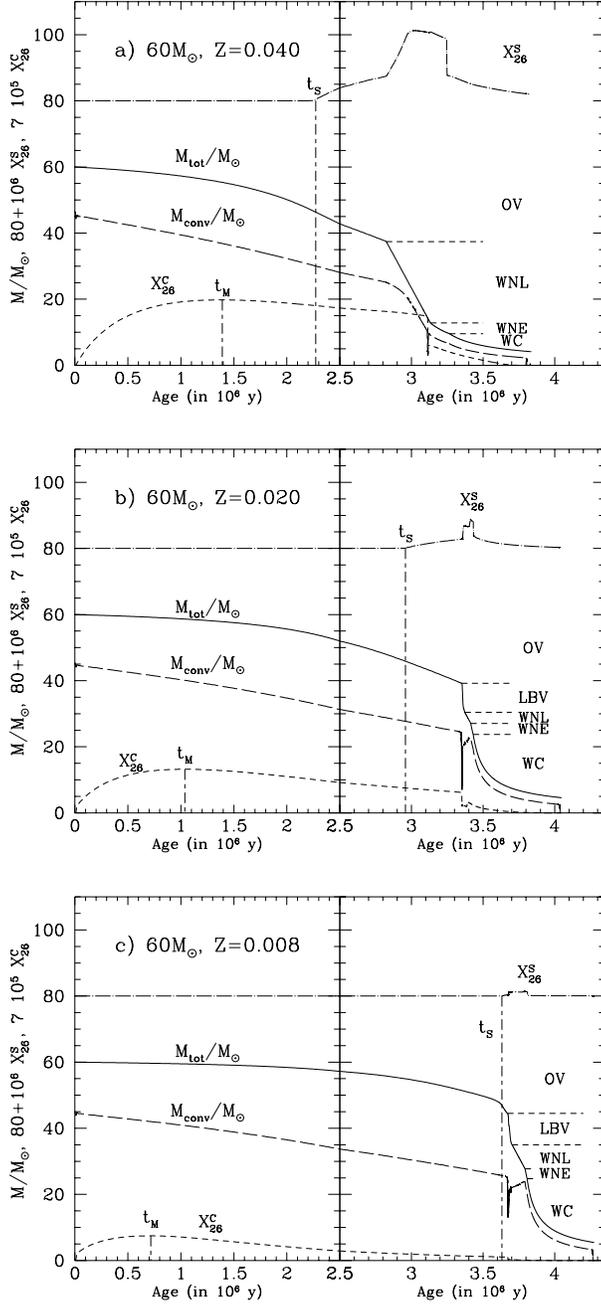
poorer and poorer in ^{26}Al as they are more external. Indeed, these cooler outer zones produce less ^{26}Al through proton captures on ^{25}Mg, while the ^{26}Al β-decay flow is temperature-independent. In other words, smaller convective cores have a tendency to admix less ^{26}Al-poor layers, and thus to keep X_{26}^c at a higher level, than more extended convective cores.

Fig. 2 complements Fig. 1 by illustrating the influence of M_i on the evolution of X_{26}^c for our $Z = 0.02$ model stars. We note in particular that $X_{26,\text{max}}^c$ is obtained earlier and reaches higher values with increasing M_i. This results directly from the fact that larger mass stars develop hotter cores, which in turn allows ^{25}Mg to be more quickly and efficiently transformed into ^{26}Al. More specifically, $X_{26,\text{max}}^c$ corresponds to 16% and 30% of the initial ^{25}Mg abundance in the 25 and 120 $M_\odot$ model stars, respectively. On the other hand, the post-maximum X_{26}^c decrease is seen to decrease less steeply with decreasing M_i. Lower mass stars indeed develop less extended convective cores, which favours a slower time decrease of X_{26}^c, as already explained above.

As displayed in Figs. 1 and 2, the ^{26}Al produced in the H-burning core appears at the stellar surface at times t_{26}^s, its mass fraction X_{26}^s building up during the WNL and WNE phases of the evolution of the WR stars. It is eventually ejected by the wind into the interstellar medium, where its β-decay contributes to the observed 1.8 MeV emission line.

As demonstrated by Figs. 1 and 2, larger X_{26}^s can be obtained with increasing Z and M_i. This trend is well in line with the M_i and Z dependence of X_{26}^c discussed above, and is strengthened further by the enhancement of the mass loss rate with M_i and Z. This indeed leads to an earlier emergence of ^{26}Al at the stellar surface, and correspondingly to a reduction of its loss by β-decay before its ejection into the interstellar medium.

At this point, let us note that a metallicity increase and the concomitant mass loss enhancement have the additional effect of decreasing the critical initial mass M_{LWR} below which the WR stage cannot be entered. This has some galactic implications to be discussed in Sect. 4.1.

All in all, one may thus conclude that an increase of Z and M_i leads to an increase of X_{26}^s in a larger and larger variety of stars.

Table 2 and Fig. 3 provide our calculated values of the mass

$$M_{26}^w(M_i, Z) = \int_0^{\tau(M_i, Z)} X_{26}^s(M_i, Z, t) \mid \dot{M}(M_i, Z, t) \mid \, \mathrm{d}t \quad (1)$$

of ^{26}Al ejected by a star of initial mass M_i and metallicity Z during the time span $\tau(M_i, Z)$ between its Zero Age Main Sequence (ZAMS) and the end of its WC-WO phase (which is in practice its presupernova stage).

The ^{26}Al yields are clearly seen to increase with M_i and Z. More specifically, a Z increase from 0.008 to 0.02 leads to a M_{26}^w enhancement by a factor between 5 and 8, depending on M_i. This increase ranges from 2 to 4 when Z goes from 0.02 to 0.04. This translates approximately into the power law expression

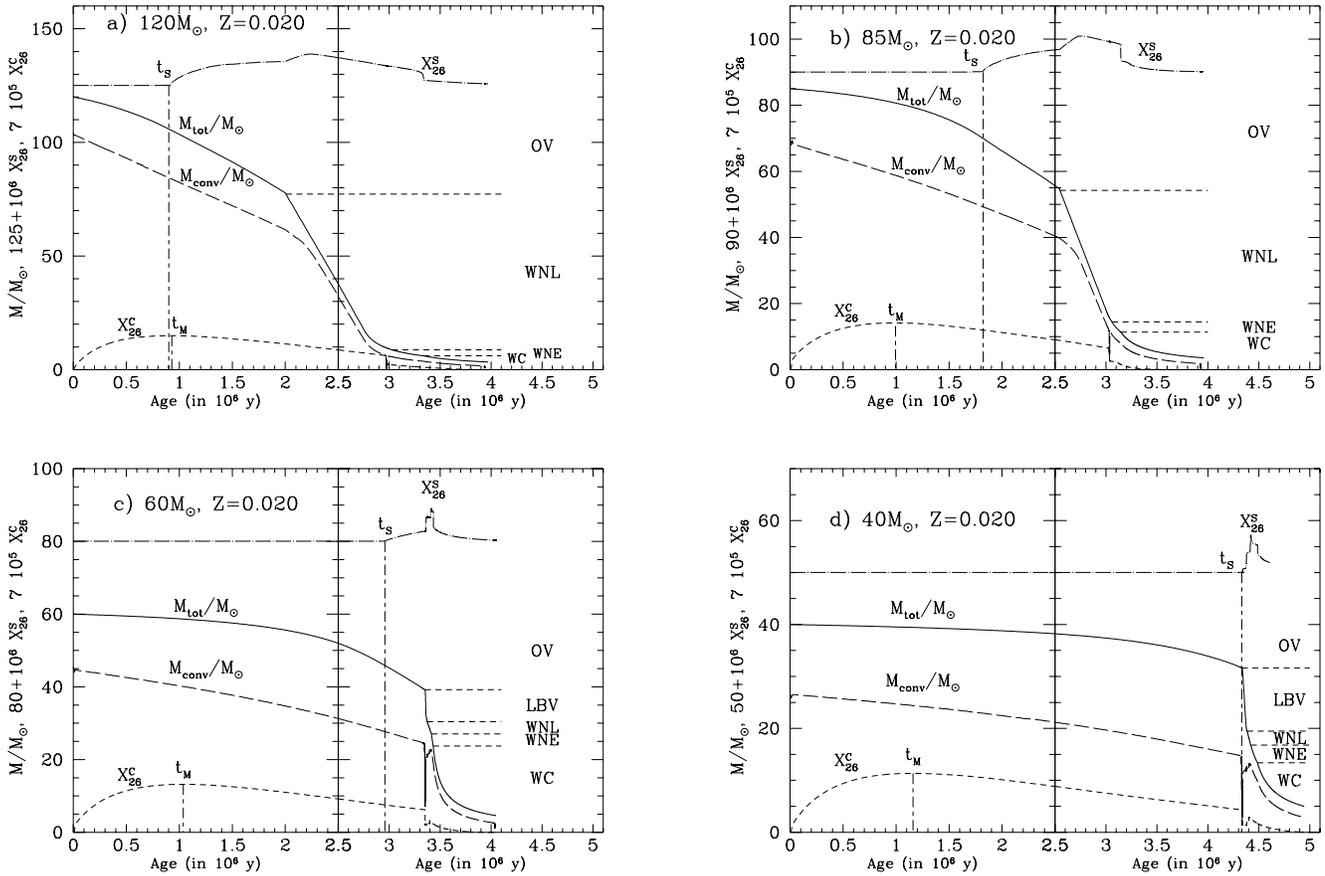$$M_{26}^w(M_i, Z) = (Z/Z_\odot)^2 M_{26}^w(M_i, Z_\odot). \quad (2)$$

Fig. 1a–c. Evolution of the total mass M_{tot}, of the mass of the convective core M_{conv}, and of the central (X_{26}^c) and surface (X_{26}^s) ^{26}Al mass fractions for the 60 $M_\odot$ model stars with metallicities $Z = 0.04$ (**a**), 0.02 (**b**) and 0.008 (**c**). The central ^{26}Al abundance reaches a maximum at time t_M. The ^{26}Al surface enrichment starts at time t_S. The various spectroscopic types encountered during the evolution are indicated on the right of the figure: OV for O-type main sequence stars, LBV for Luminous Blue Variables, WNL, WNE and WC for the different classes of WR stars (see the main text). Note the different ordinate scales defined on the left of the figure.

Fig. 2a–d. Same as Fig. 1, but for $Z = 0.02$ and $M_\text{i} = 120$ (**a**), 85 (**b**), 60 (**c**) and 40 $M_\odot$ (**d**).

This result agrees with the $(Z/Z_\odot)^2$ dependence proposed by Walter & Maeder (1989) on grounds of qualitative arguments, but predicts a weaker Z dependence than the $(Z/Z_\odot)^{2.3}$ one derived by Meynet & Arnould (1993c) from detailed computations of two 60 $M_\odot$ stellar models with $Z = 0.02$ and $Z = 0.03$ based on lower mass loss rates than the ones adopted here, as well as on different opacities and initial abundances.

For $Z = Z_\odot$, our present ^{26}Al yields are a factor of about 4 to 6 higher than those derived by Walter & Maeder (1989), and a factor of 3 larger than the ones reported by Prantzos (1991) for $Z = 0.03$ models. These increased yields mainly relate to our doubling of the mass loss rates, as discussed below.

3.2. Dependence of the yields on the mass loss rates and on the mixing prescription

A faster wind removal of the original envelope has the effect of shortening the time delay between the production of ^{26}Al in the stellar core and its ejection into the interstellar medium. This leads to an increase of the amount of ejected ^{26}Al, all other things being equal. The influence of the mass loss rates on the yields can be estimated more quantitatively by comparing the present results for the 60 $M_\odot$ model star at $Z = 0.02$ with the yields calculated by Meynet & Arnould (1993c) for the same star, but with the adoption of a two times lower mass loss rate

during the pre-WR and WNL phases[2]. This difference leads to an increase of our present yields over the previous ones by a factor of about two.

An increase of the convective core size, and thus a reduction of the envelope mass, is also expected to produce an enhanced ^{26}Al yield, as the ^{26}Al-loaded material is more readily ejected by the wind. Langer et al. (1995) have studied more quantitatively the impact of various mixing schemes on the ^{26}Al yields. In particular, they have assumed either that the boundary of the convective core is defined by the Ledoux criterion and that diffusive semiconvective mixing develops in the semiconvective zone, or that the convective core is defined by the Schwarzschild criterion with/without overshooting. They have also explored the possible role of rotation-induced mixing.

Langer et al. (1995) find that a change in the mixing scheme may affect the ^{26}Al yields for a given star by a factor of at most 3, more extended convective cores leading in general to larger yields, as expected. However, in some of the explored cases, the reverse effect is obtained. We interpret this result as the consequence of two opposite effects. On the one hand, a

---

[2] Strictly speaking, the models of Meynet & Arnould (1993c) also differ by the adopted opacities and initial abundances. These differences do not endanger the conclusion about the important impact of the selected mass loss rates.
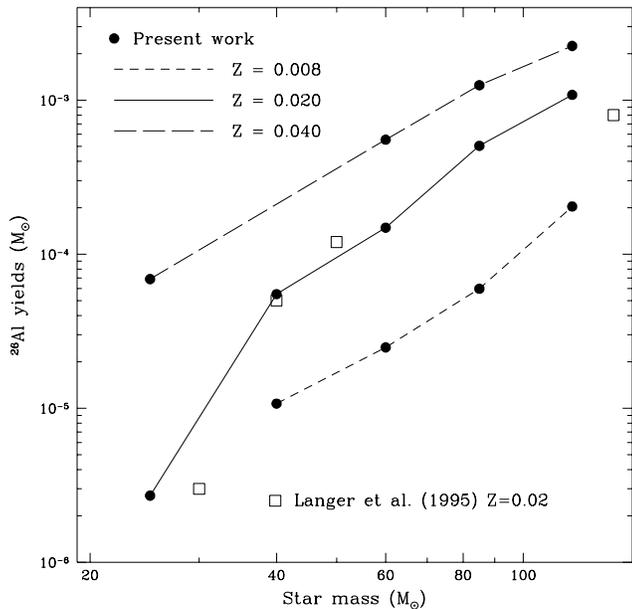
Fig. 3. Masses $M_{26}^{\rm w}(M_{\rm i}, Z)$ of ^{26}Al ejected by a star of initial mass $M_{\rm i}$ and metallicity Z = 0.008, 0.02 or 0.04 between its ZAMS and the end of its WC-WO phase. The predictions of Z = 0.02 WR models computed by Langer et al. (1995) (see main text) are also displayed for comparison.

Table 2. Wind ejected mass $M_{26}^{w}(M_{i},Z)$ of ^{26}Al in units of 10^{-4} M$_{\odot}$.

$M_{\rm i}$(M$_{\odot}$)	Z = 0.008	Z = 0.020	Z = 0.040
120	2.04	10.82	22.46
85	0.60	5.05	12.49
60	0.25	1.49	5.54
40	0.11	0.55	——
25	0.00	0.03	0.69

larger convective core favors the early appearance of ^{26}Al at the surface. On the other hand, it may increase the time lag $t_{\rm S} - t_{\rm M}$ because $t_{\rm S}$ increases as a result of longer main sequence lifetimes.

For the $Z = Z_{\odot}$ model stars, Fig. 3 shows that our yields are similar to those predicted by the models of Langer et al. (1995) computed with the standard mass loss rates of de Jager et al. (1988), the Ledoux criterion and diffusive semiconvection. At first sight, this similarity of the yields predicted from quite different models looks surprising. A plausible explanation is that a subtle balance is at work in the considered model stars between the effect of a change of $\dot{M}$ (whose enhancement increases the ^{26}Al yields) and the impact of a different mixing scheme. This comparison illustrates the intricate dependence of the ^{26}Al yields on the various physical ingredients of the models.

3.3. Effects of changes in some key nuclear reaction rates

The dependence of the WR ^{26}Al yields on the ^{25}Mg (p, γ) ^{26}Al rate has already been discussed by Prantzos (1991) and by Meynet & Arnould (1993c). Let us simply recall here that the rate proposed by Iliadis et al. (1990) is about 5 times lower than the one recommended by Caughlan & Fowler (1988) for temperatures below 80 10^6 K. In contrast to what one might conclude naively, this rate decrease leads to an enhancement of the ^{26}Al yield. A lower rate is indeed responsible for the production of ^{26}Al later in the H-burning phase, so that the time span between ^{26}Al production and wind ejection, and thus the quantity of ^{26}Al destroyed by β-decay, is reduced. According to Meynet

& Arnould (1993c), the use of the rate proposed by Iliadis et al. (1990) leads to ^{26}Al yields that are about twice higher than the ones derived for the same star with the adoption of the rate of Caughlan & Fowler (1988).

We have performed additional test computations in order to study the impact of the rate proposed by Champagne et al. (1993) for the reaction ^{26}Al (p, γ) ^{27}Si which competes with the β^+-decay destruction channel. This rate is about a factor of 6 higher than the rate of Vogelaar (1989) for a typical central temperature $T = 4 \ 10^7$ K during the H-burning phase of the considered model stars. In spite of the differences between the two predicted rates, the ^{26}Al yields change by less than 4% for stars with $M_{\rm i}$ between 60 and 120 $M_{\odot}$ and Z = 0.02 and 0.04. This convergence in the yield predictions results from the fact that the β^+-decay rate of ^{26}Al is larger than the (p, γ) rate of Vogelaar (1989) or of Champagne et al. (1993) in the derived H-burning conditions. Recently, a new estimate for the ^{26}Al (p, γ) ^{27}Si rate has been proposed (see Arnould et al. 1995). The impact of this revision and of the estimated remaining nuclear uncertainties on the ^{26}Al yields has been evaluated by Arnould et al. (1995) in the framework of parametrized astrophysical models. From this analysis, one can confidently conclude that the WR ^{26}Al yields reported here cannot be drastically affected by the use of this revisited ^{26}Al (p, γ) ^{27}Si rate.

In conclusion, the lack of a precise knowledge of the mass loss rates and the limited reliability of the mixing prescriptions are the main factors limiting the accuracy of the WR ^{26}Al yield predictions. Each of these sources of uncertainties may lead to variations in the calculated production of that radionuclide that can amount to a factor of the order of 2 to 3. In contrast, more limited uncertainties arise from a purely nuclear physics origin. Of course, important changes to the situation depicted here and associated additional uncertainties may result from mass transfer by Roche lobe overflow in close binaries, or from rotational mixing in rapidly rotating massive stars (e.g. Walter & Maeder 1989, Braun & Langer 1995, Langer et al. 1995).

In spite of the sources of uncertainties discussed above and of the possible additional intricacies eluded in this paper, the predictions of the ^{26}Al yields from other astrophysical sources are even much less secure than the WR estimates. This results from the fact that the modelling of WR stars in a stage of hydrostatic central H or He burning is much simpler than the one of asymptotic giant branch stars, novae or supernovae. Uncertainties of purely nuclear origin might also be much larger in these various types of objects than in the WR situation (see e.g.

Arnould et al. 1995 for an illustration of this statement in the case of asymptotic giant branch stars).

4. The γ-ray connection

The Comptel imaging telescope aboard the Compton Gamma-Ray Observatory (CGRO) has demonstrated that the emission of the 1.8 MeV line associated with the decay of ^{26}Al originates in rather localized regions along the galactic plane that are not necessarily concentrated in the inner disk of the Galaxy (Diehl et al. 1995a). In particular, some bright ^{26}Al emission features might be associated with the galactic inner-arm edges at $l = \pm 30°$. This might support the idea that massive stars are significant contributors to the 1.8 MeV γ-ray line, as suggested by Prantzos (1993).

On the other hand, a fraction of the 1.8 MeV emission could originate from localized foreground regions, as suggested by the recent detection of an emission peak in the direction of the Vela supernova remnant (Diehl et al. 1995b). In such conditions, as stressed by Diehl et al. (1995a), the present galactic mass M_{26}^{gal} of ^{26}Al could be lower than the canonical $2 - 3\, M_\odot$ derived from the HEAO-C (Mahoney et al. 1984) and SMM (Share et al. 1985) measurements. However, the present inability to disentangle the contributions of foreground and background sources leaves a large uncertainty on M_{26}^{gal}. In the following, we adopt $M_{26}^{\mathrm{gal}} \approx 2 M_\odot$.

4.1. Contribution of the WR population to the galactic ^{26}Al

Early estimates of the contribution of WR stars to the galactic ^{26}Al content (e.g. Prantzos et al. 1985; Prantzos and Cassé 1986) are based on an evaluation of their total number and distribution in the Galaxy. The estimate of these quantities is made uncertain by the fact that the inner galactic regions are obscured by dust, so that the WR catalogues are complete only at distances $R \lesssim 2.5$ kpc from the Sun, where $N(R) \approx 100$ WR stars have been observed up to now (van der Hucht 1995).

From an extrapolation of the data concerning the WR density in low-metallicity regions like the Large and Small Magellanic Clouds and in the solar neigborhood, the number of galactic WR stars can be roughly estimated from $N_{\mathrm{WR}} \approx N(R)(R_\odot/R)^2$, where $R_\odot = 8.5$ kpc is the galactocentric distance of the Sun. This leads to $N_{\mathrm{WR}} \approx 1100$, corresponding to a galactic frequency $f_{\mathrm{WR}} \approx 2200\, \mathrm{My}^{-1}$, since the average WR lifetime is of the order of 0.5 My. Let us note that these numbers are likely to be lower limits, since the star formation rate and the ratio of the number of WR to O-type stars increase significantly in the inner galactic regions.

An estimate of the galactic frequency of WR stars may also rely on the use of a stellar initial mass function (IMF), and on the current rate f_{SN} of massive star supernovae in the Milky Way (Prantzos & Diehl 1996). Observations of external spiral galaxies lead to the expectation that $2.5^{+0.8}_{-0.5}$ supernovae explode per century in our Galaxy, 85% of them being considered to involve massive stars (Tammann et al. 1994). From this, we assume that $f_{\mathrm{SN}} = 3$ per century. We also adopt a power-law

IMF $\Phi(M) \propto M^{-(1+x)}$ with $x = 1.5 - 2$ [Note that the value $x = 1.35$ of the Salpeter IMF was derived for $M < 10\, M_\odot$ stars. For larger masses, $x = 1.7$ seems to be more appropriate (e.g. Scalo 1986; Kroupa et al. 1993)].

In such conditions, f_{WR} relates to f_{SN} by

$$f_{\mathrm{WR}} = f_{\mathrm{SN}} \frac{\int_{M_{\mathrm{LWR}}}^{M_{\mathrm{UP}}} \Phi(M) dM}{\int_{M_{\mathrm{LSN}}}^{M_{\mathrm{UP}}} \Phi(M) dM} \approx f_{\mathrm{SN}} \left(\frac{M_{\mathrm{LWR}}}{M_{\mathrm{LSN}}} \right)^{-x}, \qquad (3)$$

where M_{LSN} and M_{LWR} are the lower limits to the masses of the stars that may become supernovae and WR. The former is $M_{\mathrm{LSN}} \approx 8 - 10\, M_\odot$, while the latter depends on the adopted mass loss rates and on metallicity. More specifically, our calculations predict that $M_{\mathrm{LWR}} \approx 25\, M_\odot$ for $Z = Z_\odot$, while $M_{\mathrm{LWR}} \approx 20\, M_\odot$ for $Z = 2\, Z_\odot$. This Z value represents a present-day average galactic metallicity if one relies on the relatively large galactic metallicity gradient $\mathrm{d}\log Z/\mathrm{d}r \approx -0.07$ dex/kpc suggested by the observations of HII regions (Shaver et al. 1983).

With these estimates, Eq. (3) leads to $f_{\mathrm{WR}} \approx (0.10 - 0.35) f_{\mathrm{SN}}$, depending on the adopted x and M_{LSN} values. This translates into 3000–10 000 WR stars per My. The lower value corresponds to $N_{\mathrm{WR}} \approx 1500$ WR stars currently present in the Galaxy, while the latter leads to the rather extreme number $N_{\mathrm{WR}} \approx 5000$. On the other hand, from the yields of Fig. 3 and our adopted IMF, an average WR yield $\langle M_{26}^{\mathrm{w}} \rangle \sim (2 - 3)\,10^{-4}\, M_\odot$ can be defined for $Z = 2\, Z_\odot$ stars.

With these estimates, the rate of ^{26}Al production by WR stars in the Galaxy amounts to

$$\dot{M}_{26}^{\mathrm{gal}} \approx 0.9 \frac{\langle M_{26}^{\mathrm{w}} \rangle}{3\,10^{-4}} \frac{f_{\mathrm{WR}}}{3000}\, M_\odot \mathrm{My}^{-1} \approx 1 M_\odot \mathrm{My}^{-1}, \qquad (4)$$

More formally, the ^{26}Al production rate from galactic WR stars may be evaluated from

$$\dot{M}_{26}^{\mathrm{gal}} = \int_0^{\mathrm{R}} 2\pi r \sigma(r)\, \mathrm{d}r \int_{M_{\mathrm{LWR}}(r)}^{120} \Phi(M) M_{26}^{\mathrm{w}}(M_i, Z, r)\, \mathrm{d}M. \quad (5)$$

In this expression, $\sigma(r)$ is the galactocentric-dependent distribution of WR stars in the Galaxy, and the dependence of M_{LWR} and of M_{26}^{w} [Eq. (1)] on the metallicity $Z(r)$ is explicitly taken into account.

The calculation of Eq. (5) is performed with the help of the following assumptions:
(1) the integral $\int_0^{\mathrm{R}} 2\pi r \sigma(r)\, \mathrm{d}r \int_8^{120} \Phi(M)\, \mathrm{d}M$ is normalized to $f_{\mathrm{SN}} = 3$ per century in the Galaxy;
(2) in the whole $1.5 \leq r \leq 15$ kpc, the metallicity gradient is $\mathrm{d}\log Z/\mathrm{d}r = -0.07$ dex kpc^{-1} under the constraint that $Z(8.5\ \mathrm{kpc}) = 0.02$. For $r < 1.5$ kpc, $Z = 0.06$;
(3) $\sigma(r)$ follows the observed surface density of giant molecular clouds as given by Scoville and Sanders (1987), except for $r < 1.5$ kpc, where 5 times lower values are adopted. This accounts for a possible overestimate of the number of H_2 molecular clouds and of the star formation rate in the central parts of our Galaxy (see Prantzos 1991).

In such conditions, Eq. (5) leads to $\dot{M}_{26}^{\mathrm{gal}} \approx 0.7 - 1.4\, M_\odot \mathrm{My}^{-1}$, in agreement with the approximate estimate provided by Eq. (4). The lower and upper limits are obtained with $x = 2$ and $x = 1.5$, respectively. These values are higher than previous estimates. For example, Signore and Dupraz (1993), Prantzos (1991, 1993) and Meynet (1994) evaluate the WR contribution to lie between 0.1 - 0.35, 0.2 - 0.5 and $0.3 - 0.9\, M_\odot \mathrm{My}^{-1}$, respectively. Our larger production rates result mainly from the higher mass loss rates considered here. Indeed, as shown in Sect. 3.2, the adoption of previously used standard mass loss rates reduces the M_{26}^{w} masses obtained here by a factor of about two. At this point, it is important to emphasize again that the choice of higher than standard mass loss rates is not arbitrary, but improves the agreement between model predictions and observations.

The mass M_{26}^{gal} of present-day galactic ^{26}Al can be obtained trivially from Eqs. (4) or (5) by noting that $M_{26}^{\mathrm{gal}} = \tau_{26} \dot{M}_{26}^{\mathrm{gal}}$ in a steady-state regime. Thus, numerically, $M_{26}^{\mathrm{gal}} \approx \dot{M}_{26}^{\mathrm{gal}}$ if M and $\dot{M}$ are expressed in $M_\odot$ and $M_\odot \mathrm{My}^{-1}$, respectively.

The preceding discussion puts forth that the estimates of M_{26}^{gal} are sensitive to the galactic metallicity gradient, the precise value of which is still uncertain. In particular, observations of B stars up to about 15 kpc from the galactic center do not confirm the existence of an important gradient (Kaufer et al. 1994, and references therein). In order to evaluate the impact of a change in the adopted $\mathrm{d}\log Z/\mathrm{d}r$ value on the predicted M_{26}^{gal}, let us assume that $Z = 0.03$ in the whole $r \leq 5.5$ kpc region. In such a case, the WR contribution amounts to $M_{26}^{\mathrm{gal}} \approx 0.4 - 0.9\, M_\odot$ if $M_{\mathrm{SN}} = 8\, M_\odot$, $x = 1.5 - 2$ and $f_{\mathrm{SN}} = 3$. The results are also directly proportional to the adopted supernova rate. If $f_{\mathrm{SN}} = 2$ instead of 3, M_{26}^{gal} is lowered from the (0.7 - 1.4) $M_\odot$ range mentioned above to about (0.5 - 0.9) $M_\odot$.

All in all, for reasonable values of the IMF, metallicity gradient, SN rate and star formation rates in the Galaxy, our stellar models predict that the contribution of the WR stars to the present-day galactic ^{26}Al production amounts to $M_{26}^{\mathrm{gal}} = 0.9 \pm 0.5\, M_\odot$. The WR stars might thus account for 20 to 70% of the approximate 2 $M_\odot$ of ^{26}Al present nowadays in the Galaxy, and are thus far from being negligible contributors.

4.2. The case of γ^2 Velorum

As already mentioned above, an enhanced 1.8 MeV γ-ray line emission has been detected in the direction of the Vela supernova remnant by the CGRO, the measured flux having values between 2.3 and $5\,10^{-5}$ cm^{-2} s^{-1} (Diehl et al. 1995b). The one steradian field of view of the instruments not only contains the Vela remnant, but also γ^2 Velorum, the nearest known WR star (WR 11). Other sources, such as the Gum nebula and novae, also lie in the same direction.

While the general 1.8 MeV emission from the Galaxy likely results from a complex population of stellar objects, this observation gives an opportunity of constraining the yield from a few stellar sources, and even possibly from a single one. Unfortunately, our ignorance of the distance(s) of the emitting source(s) makes a reliable interpretation of this observation difficult (see Oberlack et al. 1994, Prantzos & Diehl 1996).

If it is assumed that γ^2 Vel lies 300 to 450 pc away (van der Hucht 1992), and if it is considered in addition that it can be represented reasonably well by our $M_{\mathrm{i}} = 60\, M_\odot$ model star, its maximum 1.8 MeV γ-ray flux is expected to range from about 0.7 to about $1.5\,10^{-5}$ cm^{-2} s^{-1}. This falls short of accounting for the observed flux. This discrepancy might be even more severe if due consideration is taken of the fact that γ^2 Vel is a double line spectroscopic binary with a period of about 78 d (Niemela & Sahade 1980). Indeed, Braun & Langer (1995) estimate that the ^{26}Al yield from a WR star in a binary system undergoing Roche lobe overflow might be smaller than the one of a single star with the same initial mass if $M_{\mathrm{i}} \gtrsim 40\, M_\odot$, which may well be the case of γ^2 Vel.

On the other hand, if the Vela supernova remnant is located at about 500 pc, as usually estimated (Milne 1968), its 1.8 MeV γ-ray flux amounts to $0.7\,10^{-5}$ cm^{-2} s^{-1} if use is made of the ^{26}Al yield predictions of Timmes et al. (1995) for a 25 $M_\odot$ supernova with initial solar composition. This flux is comparable to the one for γ^2 Vel estimated above. However, this conclusion is quite uncertain in view of the poor knowledge of the distance of the Vela remnant and of the initial supernova mass. It has been proposed recently (Oberlack et al. 1994) that the distance to Vela may be as low as $100 - 200$ pc. In such a case, the 1.8 MeV γ-ray flux from the Vela remnant would likely exceed the one from γ^2 Vel.

In conclusion, various uncertainties prevent the unambiguous identification of the source(s) responsible for the observed γ-ray flux increase in the direction of Vela. More sensitive detectors with better angular resolution might bring some light on this interesting issue (see below).

5. Conclusions

This work presents new ^{26}Al yields from WR stars of various metallicities and initial masses. These predictions rely on new stellar models incorporating improved physical ingredients (mass loss rates, opacities, nuclear reaction rates). These models account much better than previous ones for a diversity of important observed WR properties, like luminosities, surface compositions, or number statistics.

Mainly as a result of enhanced mass loss rates, we find ^{26}Al yields larger by a factor of about two than in previous computations. We also explore quantitatively the impact on those yields of the stellar metallicity and of other uncertainties that still affect the predicted evolution of WR stars. We show that the resulting uncertainties in the ^{26}Al yields are of the order of a factor 2 - 3. These uncertainties are significantly smaller than in other potential ^{26}Al sources, like supernovae, novae, or asymptotic giant branch stars.

Finally, we calculate the contribution of the WR stars to the galactic amount of ^{26}Al under various assumptions concerning the stellar IMF, the presumed galactic metallicity gradient and supernova rate. We find that WR stars can account for about 1 $M_\odot$ of ^{26}Al during the last 10^6 y. This is about half of the

observationally derived amount. This finding suggests that WR stars may be major contributors to the present galactic ^{26}Al.

Improvements of our understanding of the galactic 1.8 MeV emission will certainly come from new γ-ray facilities. The currently tested Liquid Xenon Coded Aperture Telescope will provide a direct image of γ-ray line or continuum sources with a spatial resolution better than 2 arc minutes (Aprile et al. 1995). This instrument will greatly facilitate the identification of γ-ray sources with known stellar objects. The INTEGRAL satellite, the launch of which is scheduled for 2001, will also shed new light on the distribution of the ^{26}Al sources in the Galaxy, and will provide stringent tests of the models. This satellite will indeed be able to detect 1.8 MeV sources about five times fainter than the faintest ones observed by CGRO. If the predicted yields are correct, both the Vela supernova and the γ^2 WR star should be detectable by this instrument.

References

Abbott D.C., Conti P.S. 1987, ARAA 25, 113

Anders E., Grevesse N. 1989, Geochim. Cosmochim. Acta 53, 197

Anders E., Zinner E. 1993, Meteoritics 28, 490

Aprile E., Chupp E.L., Bolotnikov A., Dunphy P.P 1995, ApJ 453, 685

Arnould M., Mowlavi N., Champagne A. 1995, in: Stellar Evolution: What Should Be Done, Proc. of the 32nd Liège Inter. Astro. Col., eds. A. Noels, D. Fraipont-Caro, M. Gabriel, N. Grevesse, P. Demarque, Université de Liège, p. 17

Braun H., Langer N. 1995, IAU Symp. 163, Eds. K. van der Hucht & P. M. Williams, Kluwer Academic Publishers, p. 305

Caughlan G. R., Fowler W. A. 1988, Atomic Data Nuc. Data Tables 40, 283

Champagne A.E., Brown B.A., Sherr R. 1993, Nucl. Phys. A556, 123

Champagne A.E., Cella C.H., Kouzes R.T., Lowry M.M., Magnus P.V., Smith M.S., Mao Z.Q. 1988, Nucl. Phys. A487, 433

Diehl R., Dupraz C., Bennet K., Bloemen H., Hermsen W., Knödlseder J., Lichti G., Morris D., Ryan J., Schönfelder V., Steinle H., Strong A., Swanenburg B., Varendorff M., Winkler C. 1995a, A&A 298, 445

Diehl R., Bennet K., Bloemen H., Dupraz C., Hermsen W., Knödlseder J., Lichti G., Morris D., Oberlack U., Ryan J., Schönfelder V., Steinle H., Varendorff M., Winkler C. 1995b, A&A 298, L25

Giesen U., Browne C.P., Görres J., Ross J.G., Wiesher M., Azuma R.E., King J.D., Vise J.B., Buckby M. 1994, Nucl. Phys. A567, 146

Illiadis Ch., Schange Th., Rolfs C., Schröder U., Somorjai E., Trautvetter H.P., Wolke K., Endt P.M., Kikstra S.W., Champagne A.E., Arnould M., Paulus G. 1990, Nucl. Phys. A512, 509

Iglesias C.A., Rogers F.J. 1993, ApJ 412, 752

Iglesias C.A., Rogers F.J., Wilson B.G. 1992, ApJ 397, 717

de Jager C., Nieuwenhuijzen H., van der Hucht K.A. 1988, A&AS 72, 259

Jorissen A., Arnould M., 1989, A&A 221, 161

Kaufer A., Szeifert Th., Krenzin R., Baschek B., Wolf B 1994 A&A 289, 740

Kious M. 1990, Ph. D. Thesis, Université de Paris XI (unpublished)

Kroupa P., Tout C., Gilmore G. 1993, MNRAS 262, 545

Kudritzki R. P., Pauldrach A., Puls J. 1987, A&A 173, 293

Kudritzki R. P., Pauldrach A., Puls J., Voels, S. R. 1991, in: The Magellanic Clouds, IAU Symp. 148, Haynes R., Milne D. (eds.), Kluwer Acad. Publ., p. 279

Landré V., Prantzos N., Aguer P., Bogaert G., Lefebvre A., Thibaud J.P. 1990, A&A 240, 85

Langer N. 1989, A&A 220, 135

Langer N., Braun H., Fliegner J. 1995, Ap.& Sp. Sc. 224, 275

MacPherson G.J., Davis A.M., Zinner E.K. 1995, Meteoritics 30, 365

Maeder A. 1991, A&A 242, 93

Maeder A., Meynet G. 1994, A&A 287, 803

Mahoney W. A., Ling J. C., Wheaton W. A., Jacobson A. S. 1984, ApJ 286, 578

Meynet G. 1994, ApJS 92, 441

Meynet G. 1995, A&A 298, 767

Meynet G., Arnould M. 1993a, in Nuclei in the Cosmos, Käppeler F. & Wisshak K. (eds.), IOP, Bristol, p. 487

Meynet G., Arnould M. 1993b, in Nuclei in the Cosmos, Käppeler F. & Wisshak K. (eds.), IOP, Bristol, p. 503

Meynet G., Arnould M. 1993c, in Origin and Evolution of the Elements, Prantzos N., Vangioni-Flam E. and Cassé M. (eds.), Cambridge University Press, p. 540

Meynet G., Maeder A., Schaller G., Schaerer D., Charbonnel C. 1994, A&AS 103, 97

Milne D.K. 1968, Austr. J. Phys. 21, 201

Niemela V.S., Sahade J. 1980, ApJ 238, 244

Oberlack U., Diehl R., Montmerle T., Prantzos N., von Ballmoos P. 1994, ApJS 92, 443

Prantzos N. 1991, in Gamma-Ray Line Astrophysics, Durouchoux Ph. & Prantzos N. (eds), AIP, New-York, p. 129

Prantzos N. 1993, ApJ 405, L55

Prantzos N., Cassé M. 1986, ApJ 307, 324

Prantzos N., Diehl R. 1996, Phys. Rep. 267, 1

Prantzos N., Cassé M., Gros M., Doom C., Arnould M. 1985, in NASA Goddard Space Flight Center 19th Intern. Cosmic Ray Conf., Vol 1 p. 361

Scalo J. M. 1986, Fund. of Cosmic Phys. 11, 1

Schaller G., Schaerer D., Meynet G., Maeder A. 1992, A&AS 96, 269

Scoville N. Z., Sanders D. B. 1987, in: Interstellar Processes, eds. H. Thronson and D. Hollenbach (Reidel), p. 21

Share G. H., Kinzer R. L., Kurfess J. D., Forrest D. J., Chupp E. L., Rieger E. 1985, ApJ 292, L61

Shaver P. A., McGee R. X., Newton L. M., Danks A. C., Pottash S. R. 1983, MNRAS 204, 53

Signore M., Dupraz C. 1993, A&AS 97, 141

Smith L. F., Maeder A. 1991, A&A 241, 77

Tammann G., Löffler W., Schröder A. 1994, ApJS 92, 487

Timmes F. X., Woosley S. E., Hartmann D. H., Hoffman R. D., Weaver T. A., Matteucci F. 1995, ApJ 449, 204

van der Hucht K. A. 1992, A&A Rev. 4, 123

van der Hucht K. A. 1995, IAU Symp. 163, Eds. K. van der Hucht & P. M. Williams, Kluwer Academic Publishers, p. 7

Vogelaar B. 1989, Ph.D. Thesis, California Institute of Technology (unpublished)

Walter R., Maeder A. 1989, A&A 218,123

Ward R.A., Fowler W.A. 1980, ApJ 238, 266